PAPER

Terahertz absorption in graphite nanoplatelets/polylactic acid composites

View the article online for updates and enhancements.

Terahertz absorption in graphite nanoplatelets/polylactic acid composites

D Bychanok[1], **P Angelova**[2], **A Paddubskaya**[1], **D Meisak**[1], **L Shashkova**[1], **M Demidenko**[1], **A Plyushch**[1], **E Ivanov**[2], **R Krastev**[2], **R Kotsilkova**[2], **F Y Ogrin**[3] and **P Kuzhir**[1,4]

[1] Research Institute for Nuclear Problems Belarusian State University, Bobruiskaya str. 11, Minsk, 220030, Belarus
[2] OLEM, Institute of Mechanics Bulgarian Academy of Sciences, Acad. G. Bonchev str. 4, Sofia, 1113, Bulgaria
[3] University of Exeter, Exeter, EX4 4QL, United Kingdom
[4] Tomsk State University, 36 Lenin Prospekt, Tomsk 634050, Russia

E-mail: dzmitrybychanok@ya.ru

CrossMark

Abstract

The electromagnetic properties of composite materials based on poly(lactic) acid (PLA) filled with graphite nanoplatelets (GNP) were investigated in the microwave (26–37 GHz) and terahertz (0.2–1 THz) frequency ranges. The maximum of the imaginary part of the dielectric permittivity was observed close to 0.6 THz for composites with 1.5 and 3 wt.% of GNP. The experimental data of complex dielectric permittivity of GNP/PLA composites was modelled using the Maxwell-Garnett theory. The effects of fine dispersion, agglomeration, and percolation in GNP-based composites on its electromagnetic constitutive parameters, presence, and position of THz absorption peak are discussed on the basis of the modeling results and experimental data. The unique combination of conductive and geometrical parameters of GNP embedded into the PLA matrix below the percolation threshold allow us to obtain the THz-absorptive material, which may be effectively used as a 3D-printing filament.

(Some figures may appear in colour only in the online journal)

1. Introduction

Progress in the research of modern composites, as well as the achievement of very promising mechanical and electromagnetic (EM) properties, are often related to use of various types of nanostructural carbon fillers. Many researchers [1–13] showed that nanocarbon inclusions can significantly affect the EM response of composites and provide an efficient way to tune their properties in a wide frequency range. Especially in the last decade, there has been rapid development in the fields of graphene THz devices, metamaterials and absorbers [14–16].

Graphite nanoplatelets (GNPs) are very prospective and economically feasible fillers for the production of conductive composites. Particularly, recent investigations [17–24] of the EM response of GNP/polymer composites in microwave and terahertz ranges showed their great potential for the manipulation of EM radiation.

A GNP is the high aspect ratio and high conductive material having a form of thin flakes of graphite. The typical diameter and thickness of GNP-particles provided by different manufacturers vary in the range $D = 2$–20 μm, and $H = 4$–20 nm. The high aspect ratio, as well as the high electrical conductivity of GNP particles, generally define their EM properties in the microwave and THz ranges and make these carbon additives very promising for solving problems related to effective broadband absorption and shielding of EM radiation. In particular, PLA filled with GNP, carbon nanotubes, and other nanocarbons is one of the best candidates to produce layered structures or structures with different

J. Phys. D: Appl. Phys. **51** (2018) 145307

D Bychanok *et al*

sophisticated geometries via additive manufacturing (see for example [25–27]).

Recent works have showed [21, 24] that the EM properties of polymer composites based on a GNP may be effectively described in the microwave range using the Maxwell-Garnett (M-G) theory for randomly dispersed conductive ellipsoids in a dielectric matrix. The local fields, as well as the depolarization factors for ellipsoids, can be easily calculated by analytical formulae [28]. In this case, the ellipsoid is a universal particle—it may be considered in the limited case as a sphere, needle, and disk, and widely used for the prediction of EM properties of composites from statics and up to the optical range [29, 30].

In the present communication, we will consider the polymer 3D-printing suitable composites with GNP content below the percolation threshold and assume that GNP particles may be approximated as flattened conductive ellipsoids. This assumption is in good agreement with previous similar investigations in the microwave range [19, 21, 24]. Moreover, the lateral dimensions, as well as the effective conductivity of GNP particles, make them especially interesting for the terahertz frequency range. The results of simple modelling based on the M-G theory presented below predict the high absorption ability of such composites near 1 THz. A similar peak for carbon nanotube composites was predicted and experimentally observed in [31, 32].

The terahertz absorption maximum near 2.2 THz was recently observed experimentally in polyethylene-based composites with different sp^2 carbon inclusions [22], associated according to quantum chemistry calculations with particular features in the vibrational spectra of graphene. We discuss an alternative origin of the absorption peak related to the unique combination of the geometrical and conductive properties of GNPs. Moreover, in the present communication, we focus first of all on composites suitable for 3D-printing, which are particularly important for practical applications.

This paper is organized as follows: the second section describes details of modelling based on the Maxwell-Garnett theory. This formalism is then applied to explain the experimental data for the EM response of the GNP/PLA composites. The third section presents the fabrication of the composite materials and their experimental characterization. The experimental results related to the electromagnetic response of GNP/PLA composites in the microwave and terahertz ranges, comparison of the theoretical predictions and the experimental observations are presented in section 4. The last section of the manuscript is devoted to the discussion of the presented results, together with the effects of percolation and agglomeration in real composites. The conclusion part summarizes the general results most important to the further practical usage of the materials studied.

2. Maxwell-Garnett modelling

Let us consider the mixture of conductive randomly oriented ellipsoidal particles in the dielectric matrix. In the case of a low concentration of filler (below 10%), the M-G approach

[29] is often applied to predict the dielectric permittivity of such a composite material. In the classical form of M-G theory, the effective dielectric permittivity of a mixture is dependent on the dielectric permittivity of inclusions. But usually nano-carbon fillers (carbon nanotubes, onion-like carbon, GNPs, carbon black and their agglomerates) are characterized in terms of polarizability α [31, 32] (here, we use the definition of polarizability as a coefficient connecting electric field E and a dipole moment of inclusion $p = \alpha \varepsilon_0 E$, $\varepsilon_0 = 8.85 \times 10^{12}$ F m^{-1} is vacuum permittivity, where the units for polarizability are (m^3)). Throughout the paper, M-G formulas are written in terms of inclusions polarizability and the effective dielectric permittivity of a composite is [29] (all equations below were written using SI units and assume an $\exp[i\omega t - ikz]$ harmonic time convention):

$$\varepsilon_{\text{eff}} = \varepsilon_m + \frac{\frac{1}{3}\sum_{i=a,b,c} n\alpha_i/V}{1 - \frac{1}{3}\sum_{i=a,b,c}\frac{N_i n\alpha_i/V}{\varepsilon_m}}, \tag{1}$$

where ε_m is the dielectric permittivity of the matrix, n is the volume concentration of ellipsoids with semiaxes a, b, c, α_i is the polarizability of inclusions in the $i = a, b, c$ directions, N_i is the depolarization factor along the i-axis, and V is the volume of ellipsoid. The polarizability of conductive (i.e. with static conductivity σ) ellipsoid surrounded by media with the dielectric permittivity ε_m is [29]

$$\alpha_i(\nu, \sigma) = \frac{4\pi abc}{3} \frac{\varepsilon_m(1 - \frac{i\sigma}{2\pi\nu\varepsilon_0} - \varepsilon_m)}{\varepsilon_m + N_i(1 - \frac{i\sigma}{2\pi\nu\varepsilon_0} - \varepsilon_m)}, \tag{2}$$

where ν is the frequency. The depolarization factors N_i for $i = a, b, c$ directions may be calculated as [28]:

$$N_i = \frac{abc}{2} \int_0^\infty \frac{ds}{(s + i^2)\sqrt{(s + a^2)(s + b^2)(s + c^2)}}. \tag{3}$$

It is important to note again that the above presented M-G equations are written in terms of polarizability of inclusions, which is more suitable for a nanoscaled carbon filler. Nevertheless, a similar and equivalent M-G approach in terms of dielectric permittivity of inclusions was successfully applied for the prediction and description of EM properties of GNP/epoxy composites in the 8–18 GHz range [21, 24].

Due to strong dependence (see equation (2)) on the depolarization factor, the polarizability of conductive inclusion is maximal in the direction parallel to the largest lateral dimension. Particularly, the frequency dependence of polarizability $\alpha_b = \alpha_c$ of the flattened conductive ellipsoidal particle with diameter $D = 2b = 2c = 1.4$ μm, thickness $H = 2a = 17$ nm and static conductivity $\sigma = 9000$ S m^{-1} in vacuum calculated using equation (2) is presented in figure 1. The polarizability α_a have significantly smaller values in comparison with α_b, and their contribution at low frequencies (up to 5 THz) can be neglected. Below, by default, we will consider and discuss the polarizability of inclusions along the largest lateral dimension.

Let us analyse figure 1 together with equation (2). First of all, we see that in the static limit when $\nu \to 0$, the polarizability is the real number. The value of equation (2) converges to classical values of static polarizability
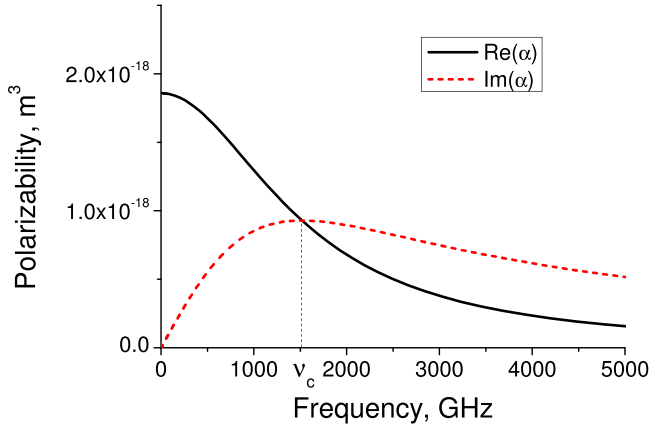
Figure 1. Frequency dependence of longitudinal complex polarizability of flattened conductive ellipsoidal particle with diameter $D = 2b = 2c = 1.4\ \mu$m, thickness $H = 2a = 17$ nm and conductivity $\sigma = 9000$ S m^{-1} in vacuum.

of the conductive particle in the external electric field parallel to the largest lateral size of the particle. For example [28], in the case of a sphere of radius R, it is $\alpha_s = 4\pi R^3$, in the case of a disk of diameter D (much larger than thickness H) $\alpha_d = 2D^3/3$, and in the case of a needle of length L (which is much larger than radius R) $\alpha_n = 4\pi L^3/(24(\ln[2L/R] - 5/3))$. It is important to note that the static polarizability is proportional to the largest lateral dimension raised to the third power, and the volume V of the particle used in equation (1) is proportional to R^3, D^2 and L in the case of spheres, disks, and needles, correspondingly. Therefore, we clearly see that the high aspect ratio particles (disks and needles) much more significantly affect the EM properties of the composite in comparison to the spheres with the same volume fraction.

Next, from examination of figure 1, we can see that the imaginary part of polarizability has a maximum at the critical frequency ν_c. Above this frequency Im(α), which is related to the Ohmic losses in conductive particles, starts to dominate. The physical origin of them is caused by the delay in the molecular polarization of filler with respect to a changing electric field in a composite medium. The trivial solve of equation $\frac{\partial}{\partial \nu}Im(\alpha_i(\nu, \sigma)) = 0$ gives the simple expression for critical frequency

$$\nu_c = \frac{N_i \sigma}{2\pi \varepsilon_0 (\varepsilon_m - \varepsilon_m N_i + N_i)}. \qquad (4)$$

According to equation (1), the maximum of Im(α) for conductive particles originates from the corresponding maximum of Im$(\varepsilon_{\text{eff}})$ in the composite. For example, for composite materials based on the spherical graphite particles ($\sigma = 120$ kS m^{-1}) in the dielectric matrix with $\varepsilon_m = 2.5$, the maximum of Im$(\varepsilon_{\text{eff}})$ is located in a very high frequency range—near 360 THz. Nevertheless, from equation (4), it is clear that by modifying the conductivity of filler, their shape and aspect ratio, it is possible to smoothly change the position of the Im$(\varepsilon_{\text{eff}})$ maximum and shift them to much lower frequencies. Particularly, the flake structure of GNP, as well as the smaller

value of conductivity ($\sim$10 kS m^{-1} [21, 24]), expects the position of the absorption maximum near 1 THz (figure 1).

It is important to note that very often the experimental data of ε for composites below the percolation threshold may be satisfactorily fitted by the Debye relaxation formula [4, 33]:

$$\varepsilon_{\text{D}} = \varepsilon_\infty + \frac{\varepsilon_s - \varepsilon_\infty}{1 + \text{i}2\pi\nu\tau}, \qquad (5)$$

where τ is the relaxation time, ε_s is the static permittivity, and ε_∞ denotes the limiting high-frequency permittivity. The fitting parameters $\tau, \varepsilon_s, \varepsilon_\infty$ are obtained from experiments. It is important to note that the expressions for dielectric permittivity ε_{eff} calculated using equation (1) and ε_D calculated using equation (5) have a similar form after simplification, and the parameters of the Debye model may be retrieved as $\varepsilon_s = \lim_{\nu \to 0} \varepsilon_{\text{eff}}(\nu)$, $\varepsilon_\infty = \lim_{\nu \to \infty} \varepsilon_{\text{eff}}(\nu)$. The relaxation time $\tau = 1/(2\pi\nu_c)$ is easy to calculate from the critical frequency ν_c.

Now let us apply equations (1) and (2) for a typical size and conductivity of GNP fillers and check how they can modify the dielectric permittivity of the composite. From the electromagnetic point of view, the most important parameters are the aspect ratio and conductivity of particles. The typical frequency dependence of the dielectric permittivity of the composite, including 1.5 wt.% of particles with conductivity $\sigma = 9000$ S m^{-1} and various aspect ratios (AR = diameter/thickness = b/a) is presented figure 2.

From figure 2(a), we can clearly see that the AR of the filler particles plays a crucial role in the EM response of the composite. The increase of AR leads to a significant increase of both components of dielectric permittivity $\varepsilon = \varepsilon' - \text{i}\varepsilon''$. For visualization of limits for ε' and ε'' obtained within the presented here modelling, the same curves are displayed in the Cole–Cole representation in the inset of figure 2(a). Additionally, in accordance with equation (4), the absorption maximum shifts to the low-frequency region.

A typical frequency dependence of the dielectric permittivity of the composite including 1.5 wt.% of particles with AR = 80 and various conductivity σ is presented in figure 2(b). From this figure, we can clearly see that a decrease in conductivity leads to a decrease of position of the Im(ε) peak. This is again the consequence of equation (4). Nevertheless, the change of σ leads to a shifting of the peak but the shape of dielectric permittivity spectra remains the same. All curves from figure 2(b) in the Cole–Cole representation are equivalent (they are plotted in figure 2(a) inset by red color). It is important to note that a possible way to change the conductivity is by doping of the carbon filler during the manufacturing process.

All theoretical observations prove the possibility to observe a terahertz absorption maximum in composites with well dispersed GNP particles inside the polymer matrix. These results are in good agreement with [22, 31, 32, 34]. Application of the presented formulae for composites with typical GNP parameters (aspect ratio, size, conductivity, etc) shows that these samples are good for terahertz absorption, due to the presence of ε'' maximum near 1 THz.

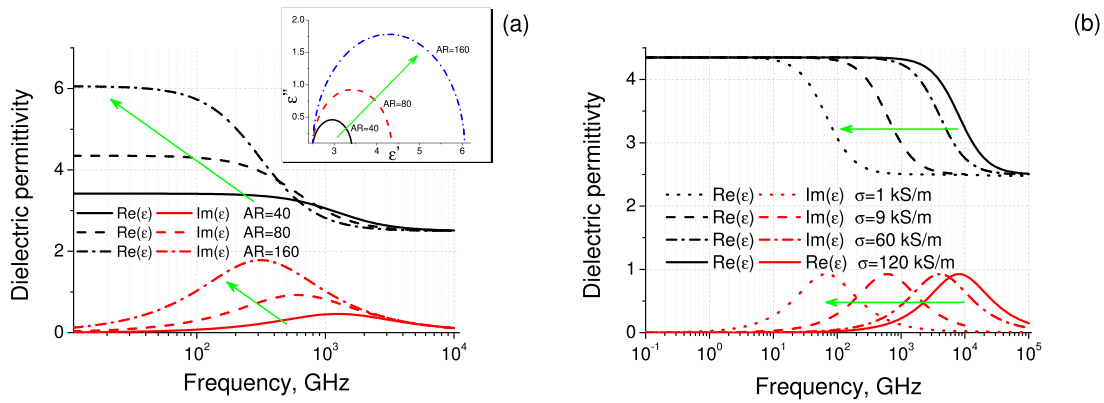J. Phys. D: Appl. Phys. **51** (2018) 145307

D Bychanok *et al*

Figure 2. (a) Frequency dependence of dielectric permittivity of composite including 1.5 wt.% of particles with conductivity $\sigma = 9000$ S m^{-1} and various aspect ratios (the green arrow shows the growth of AR from 40 to 160) (inset: the identical curves in the Cole–Cole representation). (b) The same for composite with AR = 80 and various conductivity (the green arrow shows the decrease of σ from 120 to 1 kS m^{-1}).

Table 1. The physical parameters of considered composites.

	PLA Ingeo 7001D	PLA + 1.5% GNP	PLA + 3.0% GNP
Density, g cm^{-3}	1.43	1.44	1.45
Glass-transition temperature, T_g, °C	52.1	52.1	55.0
Crystalline melt temperature, T_m, °C	144.6	144.6	145.7
Viscosity μ at $T = 200$ °C, Pa · s	1636	1731	2109

3. Fabrication of composites and their characterization

In the present communication, we used a polymer matrix suitable for further 3D printing applications. Particularly, the poly(lactic) acid polymer (PLA) Ingeo 700 1D from Nature Works, USA, was used as a matrix polymer for the preparation of composite materials samples. GNPs produced from Times Nano (TNGNPs), China, were used as fillers for the preparation of nanocomposites [35]. The source GNP-particles have a thickness in the range 4–20 nm and a diameter in the range 5–10 μm.

The samples were prepared using the following procedure. The PLA 700 1D was dissolved in chloroform in a ratio of 1:3. Suspensions of GNPs were prepared in 200 ml chloroform by ultrasonic mixing and added to the dissolved PLA. The final mixture was mechanically stirred for 60 min and dried in a vacuum oven for 24 h at 70 °C. Compositions with $\theta = 0\%$, 1.5% and 3% wt. of GNP in PLA in the form of a 1 mm thick plane parallel plate were prepared by this solution blending technique. The physical parameters, most important for further 3D printing applications of the samples under study, are presented in table 1.

The transmission electron microscopy (TEM) analysis of GNP/PLA composites was made by TEM JEOL JEM 2100 in the bright field (BF) mode at the accelerating voltage 200 kV. Results of the TEM-analysis show that the composite consists of separated GNP particles in the PLA matrix. The

typical TEM-image of the obtained composites is presented in figure 3(a). The particles have a complex multilayer-graphene-based structure, reminiscent of crumpled paper. The typical lateral size of GNP inclusion is 1–2 μm (figure 3(a)). The thickness of multilayer-graphene forming the GNP was analysed using scanning electron microscopy (SEM) (made by a S-4800 Hitachi microscope). The values of the thickness vary in the range of 5–20 nm (figure 3(b)) in good correspondence with the manufacturer data sheet [35]. Due to breaking during high power sonication treatment, the average diameter of particles was decreased to several microns. Rarely, a few agglomerates of contacting GNP particles with lateral lengths around 4–5 μm were observed at 1.5 wt% filler content.

The typical Raman spectra of GNP/PLA composites is shown in figure 4. Measurements were performed by a Raman spectrometer Nanofinder HE (LOTIS TII, Belarus-Japan) with a 600-lines/mm grating and 473 nm laser excitation. The peaks observed at 1363, 1576 and 2743 cm^{-1}, originating from the GNP, 871 and 2996 cm^{-1}, are contributed by the PLA matrix. The largest G 1576 cm^{-1} peak is typical for high ordered graphite.

The electromagnetic response of GNP/PLA composites was experimentally investigated in the Ka-band (26–37 GHz) using a scalar network analyser ELMIKA R2-408R. All measurements were carried out in a 7.2×3.4 mm waveguide system described in detail in our recent work [10]. The dielectric permittivity ε was then calculated based on the methodology described in [36].

THz measurements were carried out using a commercial THz time-domain spectrometer 'T-Spec' by EKSPLA. A 1050 ± 40 nm wave length pumping laser having a 50–150 fs pulse duration and more than 40 mW output power at approximately 80 MHz pulse repetition rate was used to excite a photoconductor antenna and produced THz radiation up to 2 THz. The spectrometer, THz emitter, and detector consist of a microstrip antenna integrated with a photoconductor (low temperature grown GaBiAs) and silicon lens. The sample in the form of a plane parallel plate was placed between the emitter and detector normally to the initial EM wave. The THz detector output is proportional to the instant electrical
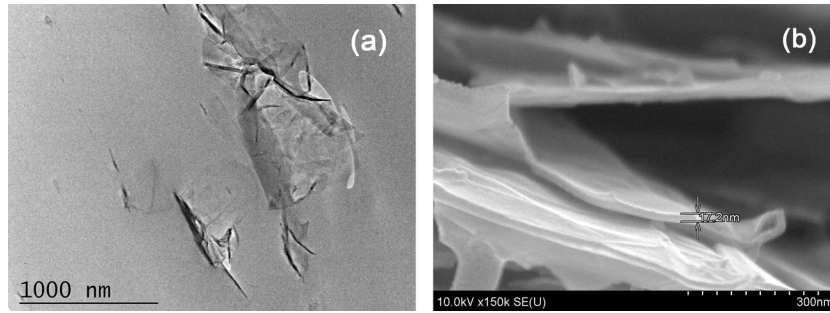
J. Phys. D: Appl. Phys. **51** (2018) 145307

D Bychanok *et al*

Figure 3. (a) TEM-image of the typical GNP-particles with lateral size about 1–2 μm in the composite material, (b) SEM-image of the side face of the GNP-particle with thickness 17.2 nm oriented parallel to the electron beam.
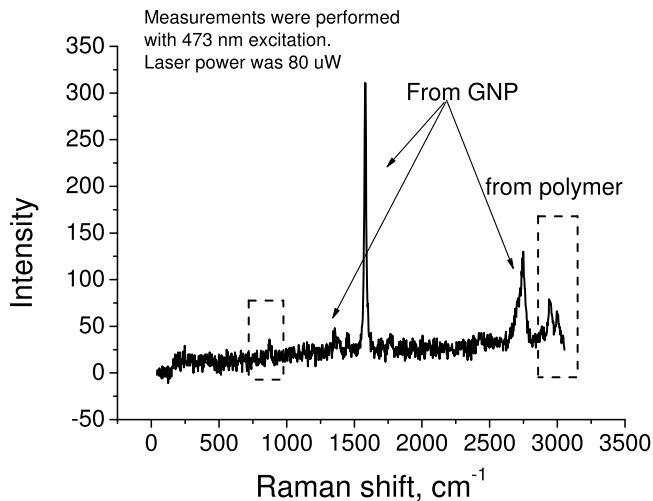

Figure 4. Raman spectra of GNP/PLA composites (arrows show peaks at 1363, 1576 and 2743 cm^{-1}, contributed by GNP, peaks 871 and 2996 cm^{-1} in a dedicated area originated by PLA).

Figure 5. Frequency dependence of composites dielectric permittivity ε obtained from experiment (scatters) and using modelling (lines) with parameters: electrical conductivity $\sigma = 9000$ S m^{-1}, GNP thickness $H = 2a = 17$ nm, GNP diameter $D = 2b = 2c = 1.4$ μm.

field strength of the THz pulse during the ultra short pumping pulse. The Fourier transform of the waveform of electrical field of the THz radiation gives the frequency dependence of the complex transmission coefficient of the investigated sample used for ε calculations [36].

4. Experimental results

The results of the calculation of the dielectric permittivity from the experimentally measured data in the microwave and THz ranges are presented in figure 5 with scatters.

First of all, the maximum of ε'' is clearly seen near $\nu_c = 0.6$ THz in figure 5. The absolute value of ε'' increases with GNP content. The real part of dielectric permittivity has a pronounced bend near 0.6 THz. The absorption coefficient of 1 mm-thick composites was about 85% at 0.6 THz.

The best fit of the experimental data using equations (1) and (2) is presented in figure 5 with lines. The following parameters of particles were used: electrical conductivity $\sigma = 9000$ S m^{-1}, GNP thickness $H = 2a = 17$ nm, and GNP diameter $D = 2b = 2c = 1.4$ μm. These parameters are in good agreement with datasheets provided by a GNP manufacturer [35] and also with other GNP-related publications [18–21, 24]. Dielectric permittivity of PLA matrix was used $\varepsilon_m = 2.5$. The
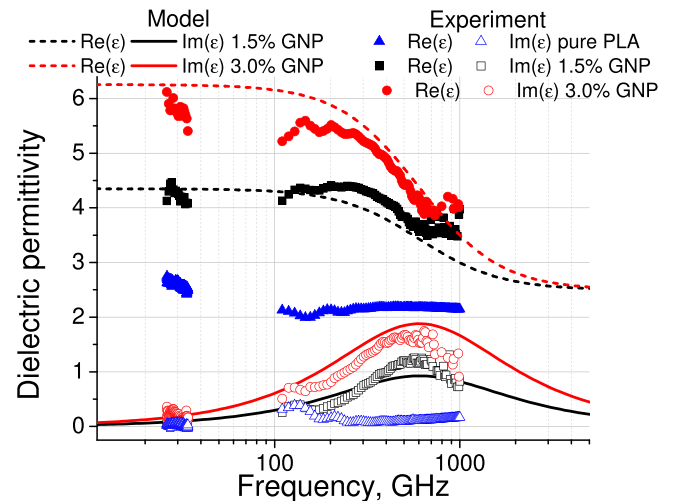
volume fraction of GNP was obtained from the mass fraction θ as $n = (1 + \frac{1-\theta}{\theta} \frac{\rho_{GNP}}{\rho_{PLA}})^{-1}$, where $\rho_{PLA} = 1430$ kg m^{-3} and $\rho_{GNP} = 2100$ kg m^{-3} are density of PLA-matrix and GNP, correspondingly.

Results of modelling are in good agreement with the experimental data. In the next section, we will discuss the general features of GNP based composites, effects of percolation and agglomeration, together with an overview and outlook for their possible practical use.

5. Discussion

As we mentioned above, the composites with GNP content below the percolation threshold were investigated. To observe THz absorption, the maximum composite should be prepared with a very high level of GNP distribution homogeneity, i.e. particles should be isolated from each other. It is very difficult to realize in practice, due to problems with the agglomeration of carbon particles [37, 38]. Additionally, at higher concentrations, the percolation occurs. The next subsection will discuss the influence of these effects on the appearance and position of the THz absorption peak.

J. Phys. D: Appl. Phys. **51** (2018) 145307

D Bychanok *et al*

5.1. Effect of agglomerates

Agglomerates and connected particles may be considered as structures with a higher aspect ratio and lower effective conductivity. The effective conductivity decreases due to the presence of contacts between particles. The agglomerates and connected particles form a percolation network with complex structured conductive regions. They may be considered as prolonged particles [21] with increased effective AR. According to equation (4), both of these parameters lead to a significant decrease of ν_c. To demonstrate the effect of agglomerates, we consider a mixture of 1.5 wt.% of the above mentioned GNP particles and 0.15% of agglomerates with diameter $D = 2b = 2c$, macroscopic length $L = 0.2$ mm and conductivity $\sigma = 3000$ S m^{-1}. In this case of the multiphase mixture, the sums in equation (1) should include terms for all fractions in the composite. The dielectric permittivity spectra for one- and two-component of agglomerates/GNP/PLA composite are presented in figure 6(a). One can see that at low frequencies, the contribution of agglomerates is dominated and in the range 5–50 GHz (see the grey region in figure 6(a)), both components are decreasing with frequency as it was observed, for example, in [19, 21, 24].

In the Cole–Cole representation (figure 6(b)), the spectra have a form of two engaged hemispheres. When the content of the filler increases, a number of agglomerates also increases. In this situation, the large hemisphere merged with the smaller one in figure 6(b) and THz peak spread and became invisible. Moreover, the contribution of the agglomerated or percolated particles will be excluded from the high-frequency absorption peak and should be taken into account at low-frequency absorption. In this case, the frequency spectra of ε will be dominated by the contribution of agglomerates and the high-frequency THz-peak will be significantly dumped. That is why it is very important to prepare well the dispersed GNP composites to observe high-frequency THz absorption phenomena. This situation was widely discussed in [21, 24], where authors used a mixture of oblate and prolate ellipsoids to explain the EM properties of similar GNP/epoxy composites at lower frequencies (8–18 GHz). Actually, from the present analysis, we can clearly see that a well dispersed GNP/PLA composite may be used as a selective THz absorber transparent for microwave radiation.

5.2. Effect of percolation

When the concentration of filler reaches the percolation threshold agglomerates or arrays of connected particles start to be comparable to the lateral dimension of the whole sample, the material starts to be conductive in DC. The description of EM processes in agglomerates is a complex problem, which may be solved within percolation theory and through applying time-consuming Monte-Carlo modelling [39].

Nevertheless, to understand the general features of broadband dielectric permittivity spectra of percolated composites, it is possible to assume that the dielectric permittivity of the matrix in percolated composites starts to be complex
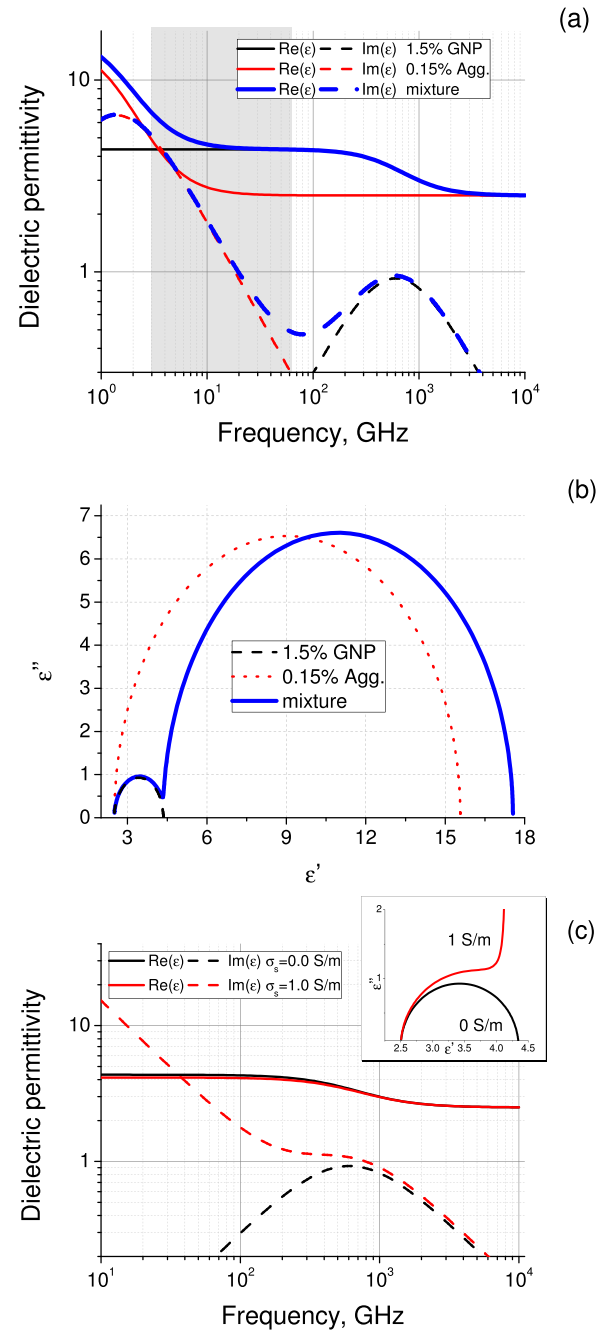
Figure 6. (a) Frequency dependence of dielectric permittivity ε of composites containing 1.5% GNP, 0.15% agglomerates, and their mixture, (b) the identical curves in the Cole–Cole representation, (c) the same as (a) for 1.5% GNP inside the matrix with and without DC conductivity σ_s (inset: the identical curves in the Cole–Cole representation).

$\varepsilon_m^* = \varepsilon_m - i\sigma_s/(2\pi\nu\varepsilon_0)$, where σ_s is the static conductivity of the composite. In this case, $\mathrm{Im}(\varepsilon_{\mathrm{eff}})$ has singularity at $\nu \to 0$. A comparison of the corresponding spectra of the composite consisting of 1.5% of GNP particles inside the neat PLA matrix and inside the matrix with dielectric permittivity ε_m^* and $\sigma_s = 1$ S m^{-1} is presented in figure 6(c). As can be seen from the figure, the percolation generally affects the imaginary part of the dielectric permittivity, whereas the real part is influenced very slightly, decreasing at low frequencies due

J. Phys. D: Appl. Phys. **51** (2018) 145307

D Bychanok *et al*

to shunting of conductive particles by the conducting matrix. The THz absorption maximum may be potentially observed in percolative composites, for small values of conductivity σ_s. Let us examine spectra from figure 6(c) in the Cole–Cole representation (see the inset of figure 6(c)). The position of the singularity is very important for the possibility of experimental THz peak observation. If σ_s is less than $\sim$1 S m^{-1}, the singularity moves to the right from the red curve and the THz peak starts to be more pronounced. If σ_s is increased then the singularity shifts to the left, and the terahertz absorption peak in that case disappears.

Summarizing this section, we can conclude that the contribution of agglomerates plays a dominate role in the formation of $Re(\varepsilon)$ at lower frequencies in percolative composites (including arrays of connected particles forming the percolation paths, agglomerates and isolated particle). The particles included to conductive paths are mainly responsible for $Im(\varepsilon)$ values and isolated particles form the THz absorption peak.

6. Conclusions

The EM properties of PLA/GNP composites were investigated in the microwave (26–37 GHz) and terahertz (0.2–1 THz) frequency ranges. We pointed out that a unique combination of conductive and geometrical parameters of GNP allow us to obtain the THz-absorptive material, which may be used as a 3D-printing filament. The preparation procedure, as well as dispersion control in this case, play crucial roles. Simple relations between the position of the absorption maximum and geometrical and conductive parameters of inclusions were derived on the basis of M-G modelling. An absorption maximum was experimentally observed near a frequency of 0.6 THz for the GNP/PLA composites with 1.5 and 3 wt.% of graphite fillers, which is below the percolation threshold. The experimental data were fitted using M-G formulae. Effects of percolation and agglomeration in GNP-based composites were discussed in view of responsibility for electromagnetics constitutive parameters of the GNP comprising composites and the position of the THz absorption peak.

Acknowledgments

ORCID iDs

D Bychanok https://orcid.org/0000-0002-7055-4274
P Kuzhir http://orcid.org/0000-0003-3689-0837

References

[1] Qin F and Brosseau C 2012 A review and analysis of microwave absorption in polymer composites filled with carbonaceous particles *J. Appl. Phys.* **111** 061301–24

[2] Brosseau C, Molinie P, Boulic F and Carmona F 2001 Mesostructure, electron paramagnetic resonance, and magnetic properties of polymer carbon black composites *J. Appl. Phys.* **89** 8297–310

[3] Kuzhir P *et al* 2011 Microwave probing of nanocarbon based epoxy resin composite films: toward electromagnetic shielding *Thin Solid Films* **519** 4114–8

[4] Bychanok D, Kuzhir P, Maksimenko S, Bellucci S and Brosseau C 2013 Characterizing epoxy composites filled with carbonaceous nanoparticles from dc to microwave *J. Appl. Phys.* **113** 124103–6

[5] Sedelnikova O, Kanygin M, Korovin E, Bulusheva L, Suslyaev V and Okotrub A 2014 Effect of fabrication method on the structure and electromagnetic response of carbon nanotube/polystyrene composites in low-frequency and ka bands *Compos. Sci. Technol.* **102** 59–64

[6] Gradoni G, Micheli D, Mariani Primiani V, Moglie F and Marchetti M 2013 Determination of the electrical conductivity of carbon/carbon at high microwave frequencies *Carbon* **54** 76–85

[7] Suslyaev V I, Kuznetsov V L, Zhuravlev V A, Mazov I N, Korovin E Y, Moseenkov S I and Dorozhkin K V 2013 An investigation of electromagnetic response of composite polymer materials containing carbon nanostructures within the range of frequencies 10 MHz 1.1 THz *Russ. Phys. J.* **55** 970–6

[8] De Vivo B, Lamberti P, Tucci V, Guadagno L, Vertuccio L, Vittoria V and Sorrentino A 2012 Comparison of the physical properties of epoxy based composites filled with different types of carbon nanotubes for aeronautic applications *Adv. Polym. Technol.* **31** 205–18

[9] Yu A, Ramesh P, Itkis M E, Bekyarova E and Haddon R C 2007 Graphite nanoplatelet/epoxy composite thermal interface materials *J. Phys. Chem.* C **111** 7565–9

[10] Bychanok D *et al* 2016 Exploring carbon nanotubes/BaTiO$_3$/ Fe$_3$O$_4$ nanocomposites as microwave absorbers *Prog. Electromagn. Res.* C **66** 77–85

[11] Kuzhir P *et al* 2013 Epoxy composites filled with high surface area-carbon fillers: optimization of electromagnetic shielding, electrical, mechanical, and thermal properties *J. Appl. Phys.* **114** 164304

[12] Kranauskaite I *et al* 2014 Dielectric properties of graphite-based epoxy composites *Phys. Status Solidi* a **211** 1623–33

[13] Plyushch A, Macutkevic J, Kuzhir P P, Banys J, Fierro V and Celzard A 2015 Dielectric properties and electrical conductivity of flat micronic graphite/polyurethane composites *J. Nanophoton.* **10** 012511

[14] He X, Gao P and Shi W 2016 A further comparison of graphene and thin metal layers for plasmonics *Nanoscale* **8** 10388–97

[15] He X, Zhong X, Lin F and Shi W 2016 Investigation of graphene assisted tunable terahertz metamaterials absorber *Opt. Mater. Express* **6** 331–42

[16] He X 2015 Tunable terahertz graphene metamaterials *Carbon* **82** 229–37

[17] Li J, Kim J-K and Sham M L 2005 Conductive graphite nanoplatelet/epoxy nanocomposites: effects of exfoliation and UV/ozone treatment of graphite *Scr. Mater.* **53** 235–40

[18] Hung M-T, Choi O, Ju Y S and Hahn H 2006 Heat conduction in graphite-nanoplatelet-reinforced polymer nanocomposites *Appl. Phys. Lett.* **89** 023117

[19] Lee S-E, Choi O and Hahn H T 2008 Microwave properties of graphite nanoplatelet/epoxy composites *J. Appl. Phys.* **104** 033705

[20] Liu H L, Carr G, Worsley K, Itkis M, Haddon R, Caruso A, Tung L and Wang Y 2010 Exploring the charge dynamics in graphite nanoplatelets by thz and infrared spectroscopy *New J. Phys.* **12** 113012

[21] Sarto M S, D'Aloia A G, Tamburrano A and De Bellis G 2012 Synthesis, modeling, and experimental characterization of graphite nanoplatelet-based composites for EMC applications *IEEE Trans. Electromagn. Compat.* **54** 17–27

[22] Chamorro-Posada P, Vazquez-Cabo J, Rubinos-Lopez O, Martin-Gil J, Hernandez-Navarro S, Martin-Ramos P, Sanchez-Arevalo F M, Tamashausky A V, Merino-Sanchez C and Dante R C 2016 THz TDS study of several sp^2 carbon materials: graphite, needle coke and graphene oxides *carbon* **98** 484–90

[23] Plyushch A, Macutkevic J, Kuzhir P, Banys J, Bychanok D, Lambin P, Bistarelli S, Cataldo A, Micciulla F and Bellucci S 2016 Electromagnetic properties of graphene nanoplatelets/epoxy composites *Compos. Sci. Technol.* **128** 75–83

[24] Marra F, D'Aloia A G, Tamburrano A, Ochando I M, De Bellis G, Ellis G and Sarto M S 2016 Electromagnetic and dynamic mechanical properties of epoxy and vinylester-based composites filled with graphene nanoplatelets *Polymers* **8** 272

[25] 3D black magic filament www.blackmagic3d.com/conductive-graphene-3d-printing-pla-filament-p/grphn-175.htm

[26] Paddubskaya A *et al* 2016 Electromagnetic and thermal properties of three-dimensional printed multilayered nano-carbon/poly(lactic) acid structures *J. Appl. Phys.* **119** 135102

[27] Kotsilkova R *et al* 2017 Mechanical and electromagnetic properties of 3D printed hot pressed nanocarbon/poly(lactic) acid thin films *J. Appl. Phys.* **121** 064105

[28] Landau L D and Lifshitz E 1960 *Electrodynamics of Continuous Media* (*Course of Theoretical Physics* vol 8) (Oxford: Pergamon)

[29] Priou A 1992 *Dielectric Properties of Heterogeneous Materials* vol 6 (Amsterdam: Elsevier)

[30] Bohren C F and Huffman D R 2008 *Absorption and Scattering of Light by Small Particles* (New York: Wiley)

[31] Shuba M V, Melnikov A V, Paddubskaya A G, Kuzhir P P, Maksimenko S A and Thomsen C 2013 Role of finite-size effects in the microwave and subterahertz electromagnetic response of a multiwall carbon-nanotube-based composite: theory and interpretation of experiments *Phys. Rev.* B **88** 045436

[32] Slepyan G Y, Shuba M V, Maksimenko S A, Thomsen C and Lakhtakia A 2010 Terahertz conductivity peak in composite materials containing carbon nanotubes: theory and interpretation of experiment *Phys. Rev.* B **81** 205423

[33] Jonscher A K 1999 Dielectric relaxation in solids *J. Phys. D: Appl. Phys.* **32** R57

[34] Ju L *et al* 2011 Graphene plasmonics for tunable terahertz metamaterials *Nat. Nano* **6** 630–4

[35] www.timesnano.com/en/view.php?prt=3,36,65,104

[36] 2009 Standard test method for measuring relative complex permittivity and relative magnetic permeability of solid materials at microwave frequencies, ASTM D5568-08

[37] Shuba M, Paddubskaya A, Kuzhir P, Maksimenko S, Ksenevich V, Niaura G, Seliuta D, Kasalynas I and Valusis G 2012 Soft cutting of single-wall carbon nanotubes by low temperature ultrasonication in a mixture of sulfuric and nitric acids *Nanotechnology* **23** 495714

[38] Shuba M, Maksimenko S and Lakhtakia A 2007 Electromagnetic wave propagation in an almost circular bundle of closely packed metallic carbon nanotubes *Phys. Rev.* B **76** 155407

[39] Spinelli G, Giustiniani A, Lamberti P, Tucci V and Zamboni W 2012 Numerical study of electrical behaviour in carbon nanotube composites *Int. J. Appl. Electromagn. Mech.* **39** 21–7